JOURNAL OF MATERIALS SCIENCE 6 (1971) 1479–1485

An investigation of the Substructural Changes Accompanying High-Temperature Creep of Mono- and Polycrystalline Nickel Samples

E. E. BADIYAN, A. F. SIRENKO
Solid State Physics Department, Kharkov State University, USSR

Results are presented here of an investigation of the kinetics of high-temperature creep of mono- and polycrystalline nickel samples and of the associated substructural changes. It is shown that at low stresses, not exceeding the so-called linear creep limit p_0, creep takes place according to the Nabarro-Herring mechanism. The characteristic particle size allowed for in the Nabarro-Herring theory is similar to the size of the blocks (subgrains), measured by X-ray diffraction. In the first stage of creep at stresses $p < p_0$ the average block size increases and the dislocation density decreases. In the second and third stages the creep does not cause any noticeable changes in the substructural characteristics (block size, dislocation density). Creep of the material is accompanied by the onset of porosity, the formation and development of which is due, apparently, to the coalescence of vacancies.

At $p > p_0$, when Weertman's mechanism is the main creep mechanism, the dislocation density increases with increase in the amount of creep. Creep in this stress range is accompanied by the appearance of pore-cracks which are formed mainly at the grain (block) boundary junctions; these hinder the movement of dislocations.

The dependence of the linear creep limit on temperature is determined by the temperature-dependence of the shear modulus.

1. Introduction

The high temperature creep of metals and alloys may occur by essentially different mechanisms depending on the applied stress and testing temperature [1, 2]. At high temperatures and low stresses the Nabarro-Herring diffusion mechanism [3, 4] applies; this mechanism is a non-threshold mechanism and creep may occur at arbitrarily low stresses. For example, so-called "negative" creep has been observed [5] at temperatures below the melting point in the absence of an external load (owing to surface tension forces). The diffusion creep rate is determined by the flow of vacancies from sources to sinks and varies linearly with stress.

At stresses exceeding some threshold value of p_0 (linear creep limit), which is necessary to overcome the barriers restricting the movement of dislocations, the greater part of the creep is determined by the displacement of dislocations in their slip planes. In this case, the rate-controlling mechanism is a diffusion process, but the laws of dislocation-creep (dependence of steady-state creep rate on stress, grain size, preliminary cold deformation, etc.) differ markedly from those which apply to pure diffusion-creep.

The kinetics of both diffusion- and dislocation-creep are determined, essentially, by the structural and substructural characteristics of the metal, which, in their turn, may change noticeably during creep. In this connection it is of interest to observe directly the nature of the structural changes accompanying creep at temperatures and stresses covering the region of pure diffusion-creep and the region where different deformation mechanisms are superimposed. Data are presented below which show the changes in the blocks and dislocation

structures at stresses $p < p_0$ and $p > p_0$ for monocrystalline and polycrystalline nickel samples; nickel is a suitable material for this series of investigations since it has high linear creep limits.

2. Experimental Method

High-purity nickel (99.99 %) was used to prepare the paddle-shaped samples (60 mm long and cross-section of the test length 1 × 10 mm²). Before testing, the samples were exposed to a recrystallisation-anneal at temperatures 5 to 10° below the melting point, forming either single crystals or coarse-grained samples (single grains spanning the thickness). Creep tests were carried out in vacuum at 1000 to 1250° C and at stresses of 20 to 400 g/mm². A diagram of the apparatus is shown in fig. 1.

A highly sensitive inductive tensometer [6], whose design is based on the transformer principle, was used to measure low creep values. The tensometer transducer consists of three windings on one coil, one of which is the primary, the other two the secondary windings. Each of the windings contains 800 turns of 0.09 mm diameter copper wire. The Armco-iron core (20) moves inside the coil; the core is joined by a connecting rod (3) and clamp (2) to the sample (1). The core is moved vertically by rotating a conical ground joint (4); this displacement is converted into a translational movement of the sample. The core and the windings are surrounded by an Armco-iron screen (16). The primary winding of the transducer is fed by a high frequency sinusoidal voltage (15 kHz). The difference signal set up in the secondary circuit on moving the core is fed to the input of an amplifier. A recording potentiometer, which registers the deformation of the sample, is connected in parallel to the measuring instrument of the amplifier. The width of the linear section of the transducer characteristics along the displacement axis is 10 mm, the strength of the residual signal is 0.2 mV, and the power consumption 1.5 W. The sensitivity threshold of the tensometer is ~ 0.2 μm.

The temperature of the sample was measured and recorded with a potentiometer. The temperature during the tests was maintained within $\pm$ 1° C limits.

To determine the characteristics of the block structure of the samples, various modifications of the X-ray diffraction method were used. For a sample with a fine-block structure the average

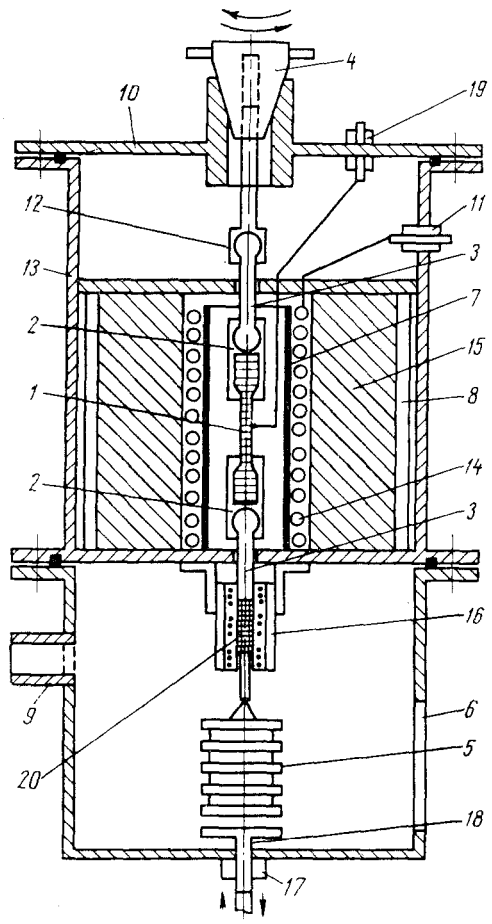

Figure 1 Schematic diagram of apparatus for studying creep. 6, viewing window; 7, aluminium oxide tube; 8, screen; 9, nozzle for evacuation; 10, cover of casing; 11, vacuum inlet for heater; 12, clamp for quartz connecting rod; 13, casing; 14, heater windings; 15, refractory brick; 16, inductive transducer; 17, vacuum seal; 18, rod; 19, vacuum inlet for thermocouples. For other notations see text.

block size (L) was determined by a method proposed in [7].

Chemical etching was used to clarify the dislocation structure (determination of the dislocation density N). Etch pits were most clearly detected using a solution of Cu ions in concentrated nitric acid as the etching agent (1 part of concentrated nitric acid, saturated with copper, was mixed with 4 to 5 parts of pure concentrated HNO_3).

To avoid possible changes in the dislocation distribution when the sample was cooled from high temperatures, loads applied to the sample

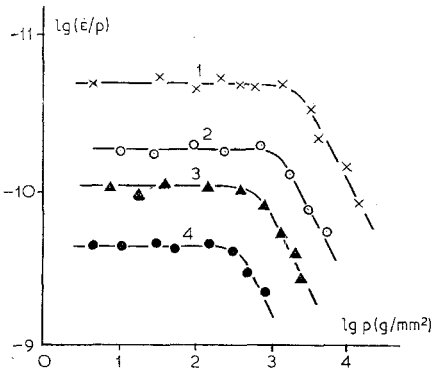

Figure 2 Dependence of the ratio $\dot{\epsilon}/p$ on p for Ni samples. Temperature: 1000°C-(1); 1100°C-(2); 1200°C-(3); 1300°C-(4). Ordinate: $\log_{10}(\dot{\epsilon}/p)$. Abscissa: $\log_{10}p(g/mm^2)$.

during testing were only removed at room temperature. Control experiments showed that under such cooling conditions the dislocation distribution is practically unchanged. Typical photomicrographs of etch figures, corresponding to different stages of creep, are shown in figs. 3 and 4.

The X-ray diffraction method was used as well as chemical etching to determine the dislocation density ρ.* According to reference [9] the broadening of reflections from separate grains, caused by the presence of dislocations, is determined from the expression

$$(2\Delta\theta)^2 = k\rho\mathbf{b}^2 \tan^2 2\theta \log_e\left[\sqrt{\frac{\pi\rho}{12}} R \log_e \sqrt{\frac{\pi\rho}{12}} R\right] \quad \ldots\ldots (1)$$

where ρ is the dislocation density, $\mathbf{b}$ is the Burgers vector, θ is the Bragg angle and k is a factor which is constant for a given reflection (determined by the indices of the reflecting plane and the value of Poisson's ratio); for the (002) reflection of Ni in Fe_{K_α} radiation it is about 0.018. R is a characteristic parameter of the dislocation distribution in the crystal (see [9] for

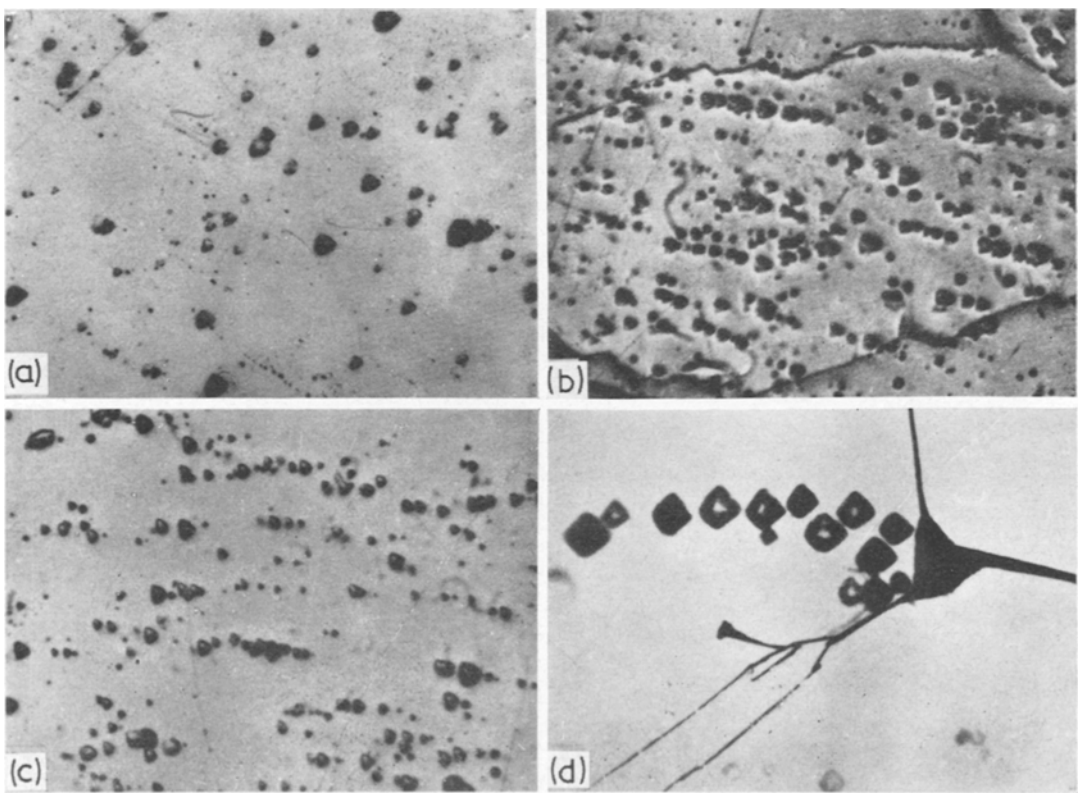

Figure 3 Dislocation structure of Ni after a prolonged high temperature anneal (10 h at 1440°C) (a); and after creep tests at 1200°C at a stress of 15 kg/cm² for 2 h (b); 8 h (c); and 19 h (d). Magnification: a, b, c (× 160), d (× 750).

*The symbols ρ and N are used for dislocation density, measured by X-ray diffraction (ρ) and etch pit density (N), since ρ and N may differ in value (see table I).

details). A calculation [10] gives $R \simeq 1$ to 2×10^{-4} cm; it is possible of course, that the true values differ from the calculated values mentioned above, but since $\log_e R$ occurs in equation 1 this approximation is permissible. In fact, a comparison of the values of ρ and N

TABLE I Change in dislocation density ρ, average block size L, and etch pit density N of polycrystalline and monocrystalline Ni samples during creep at 1200° C.

Type of sample	Deformation period, h	Applied stress, g/mm²	Block size (μm) measured by X-ray diffraction, L	Dislocation density, ρ cm^{-2}	Etch pit density, N cm^{-2}
Polycrystal	0	50	8	7.10^5	3.10^5
	8	50	10	3.10^5	2.10^5
	24	50	11	2.10^5	1.10^5
	0	280	9	6.10^5	3.10^5
	8	280	5	2.10^6	1.10^6
	15	280	4	1.10^6	1.10^6
Single crystal	0	50	12	3.10^5	1.10^5
	12	50	15	1.10^5	8.10^4
	8	260	8	8.10^5	5.10^5
	16	260	3	2.10^6	6.10^5

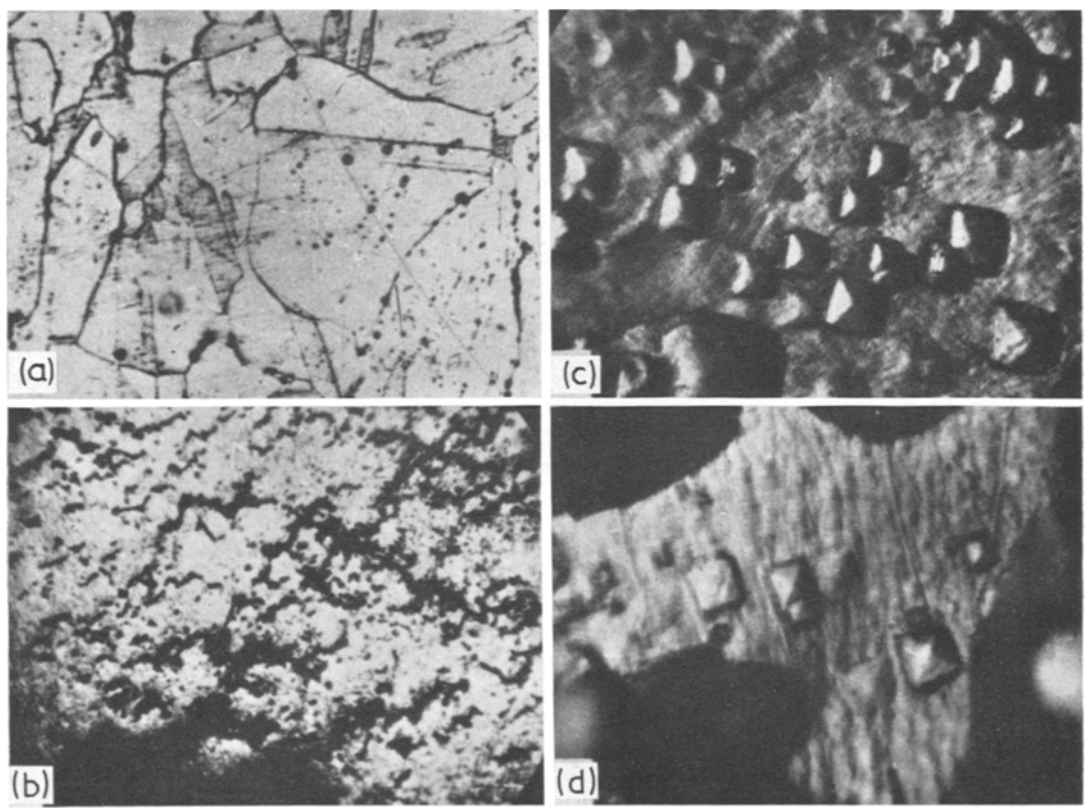

Figure 4 Development of porosity during creep of poly-crystalline Ni at 1200° C and a stress of 9.5 kg/cm². (a) after testing for 12 h; (b) as in (a), etching on dislocation; (c) after testing for 135 h; (d) as in (c), etching on dislocation. Magnification: a, c (× 160); b, d (× 840).

showed a satisfactory correlation between them (see table I). The differences (by a factor of up to about 3) can be explained satisfactorily since, in chemical etching, outcrops of dislocations are exposed which are mainly decorated with impurity atoms. This is supported by the fact that $\rho \geqslant N$ for all the samples studied.

3. Experimental Results and Discussion

The essential criterion of the mechanism of high-temperature creep is the dependence of the steady-state creep rate $\dot{\epsilon}$ on the applied stress p. When creep occurs by the Nabarro-Herring mechanism [3, 4], this dependence is linear; for dislocation-creep $\dot{\epsilon} \propto p^n$ where $n > 1$ [14].

The experimental data shown in fig. 2, where $\log_{10} \dot{\epsilon}/p$ is plotted against $\log_{10} p$, characterise the dependence of $\dot{\epsilon}$ on p for polycrystalline nickel samples tested at 1100 to 1350°C. After a preliminary high temperature anneal (8 to 12 h at 1440°C) all the samples had, in the initial state, an average linear grain size of 2 mm and a relatively low dislocation density (1 to 3 × 10^5 cm^{-2}).

As is shown in fig. 2 at each test temperature there is a stress range, $0 < p < p_0(T)$, in which $\dot{\epsilon}/p$ is almost independent of p, i.e. $\dot{\epsilon}$ varies linearly with p. According to the results of the metallographic and X-ray structure investigations, the creep at $p < p_0$ is not accompanied by any significant change in the dislocation structure Both in the initial state and after creep tests a fairly uniform distribution of dislocations is observed over the bulk of the crystal (or separate grain in a polycrystalline sample) (see fig. 3). A small decrease in the dislocation density and increase in the average size of the subgrain can be seen in the initial stages of creep. These changes in subgrain size are more pronounced at higher levels when the sample has a more highly distorted crystal lattice. For samples subjected to a prolonged high-temperature anneal (several tens of hours at 1440°C) the transient creep stage (at $p < p_0$) is almost non-existent in the creep curves and there are no noticeable changes in the substructural characteristics.

A quantitative treatment of the results obtained showed (table I) that at stresses $p < p_0$ there is fairly close agreement between values for the steady-state creep rate $\dot{\epsilon}_{exp}$ (measured experimentally) and those calculated from Herring's formula $\dot{\epsilon}_H$:

$$\dot{\epsilon}_H = \frac{AD\Omega}{kT} \cdot \frac{p}{L^2}, \qquad (2)$$

where D is the self-diffusion coefficient, Ω is the atomic volume, k is the Boltzmann constant, T is the absolute temperature, L is the characteristic size and A is a coefficient depending on the shape of the block. In the absence of any pronounced anisotropy in the form of the subgrains, A can be considered to be constant. In our calculations it was taken as equal to unity.

In calculating values of $\dot{\epsilon}_H$ from formula 2, equilibrium values of the self-diffusion coefficient of nickel were used and the average size of the subgrain (L), measured by X-ray diffraction, was taken as the characteristic size.

Owing to the linear dependence of $\dot{\epsilon}$ on p (for $p < p_0$) and the similarity in the values of $\dot{\epsilon}_H$ and $\dot{\epsilon}_{exp}$, it can be concluded that the Nabarro-Herring mechanism is the main creep mechanism in this stress range. At stresses not exceeding the linear creep limit there was no noticeable increase in the dislocation density even in the tertiary stage of creep preceding fracture of the sample. Photomicrographs are shown in fig. 4 of a nickel sample tested at 1200°C and at a stress of 9.5 kg/cm². The development of pores during the creep process, which causes the sample to fracture, can be clearly seen in the photographs; however, there is no noticeable change in the dislocation density during the whole test period (up to fracture).

The pores formed during creep at stresses $p < p_0$ are circular and appear both at the grain boundaries and inside the crystal; for monocrystalline samples they are located mainly at the subgrain boundaries. In this case, as is seen, for example, in fig. 5, where the average pore radius $\bar{r}$ is shown as a function of the testing time, the relationship $\bar{r} \propto t^{\frac{1}{2}}$ applies, indicating that pore growth in the high temperature creep of Ni at

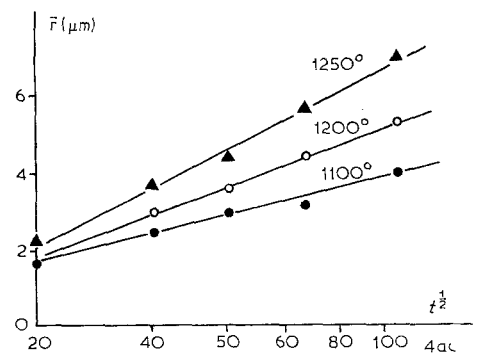

Figure 5 Change in the average pore radius $\bar{r}$ during creep of Ni at 1100°C, 1200°C and 1250°C at a stress of 9.5 kg/cm². Ordinate: $\bar{r}(\mu m)$. Abscissa: $\sqrt{t}$(h).

low stresses occurs by a diffusion mechanism. The change in slope of the straight lines corresponding to $\bar{r} = f(\sqrt{t})$, on varying the testing temperature, is in good agreement with the temperature dependence of the self-diffusion coefficient of Ni. On the basis of the vacancy mechanism of pore growth (dissolution), the change in the linear dimensions of a pore (we consider it in the first approximation as a sphere of radius r) may be described by the expression

$$\frac{dr}{dt} = \frac{1}{4\pi r^2} Q\Omega \approx \frac{D\Omega}{kT},$$

where $Q = D_b \nabla c$ is the flux of vacancies arriving at the pore, D_b and c are the diffusion coefficient of the vacancies and their concentration, respectively. At $r < r_{Cr} = 2\sigma/p$ the pore must contract in size (sinter) and the embryo pore will only grow if it reaches the critical size r_{Cr} as a result of fluctuations. These considerations agree in particular with the fact that at any stage of creep only pores of quite large sizes ($\sim 10^{-4}$ to 10^{-5} cm and above) are generally observed.

Qualitatively different mechanisms are observed in the creep process at stresses above the linear creep limit. A series of photomicrographs are shown in fig. 3 of the dislocation structure of Ni samples in the initial state and in different stages of creep at 1200°C and a stress of 15 kg/cm². In the steady-state stage of creep there is an increase in the density of dislocations; these are no longer located uniformly throughout the bulk of the crystal (grain), as in the initial state, but mainly in definite slip planes. Groups of dislocations, hindered by obstructions, can be clearly seen. Fig. 3 shows the development of a crack at a pore at the junction of intergranular boundaries (which constitute one type of obstacle to the movement of dislocations in the slip planes). In this case the pore-crack is wedge-shaped, rather than round.

Multiplication of dislocations under high-temperature creep conditions at $p > p_0$ causes reduction in size of the blocks; this happens mainly at the stage of transient creep. During steady-state creep the dislocation density and the size of the blocks, measured by X-ray diffraction, were practically unchanged (table I).

The data indicate that there is a fairly wide range of stresses at high temperatures where the Nabarro-Herring diffusion mechanism is the dominant mechanism in the development of creep. The extent of this range appears to be determined by the temperature dependence of the shear modulus. In fact, the linear creep limit p_0 corresponds to a stress at which dislocation loops can generate new dislocations. The latter is given approximately by $(G|\mathbf{b}|)/l$ [11], where $\mathbf{b}$ is the Burgers vector and l is the distance between anchored points of dislocation loops. If we assume that $p_0 \simeq (G|\mathbf{b}|)/l$ then taking into account the temperature dependence of the shear modulus G for Ni [12] values are obtained for l which are close to the block sizes, measured by X-ray diffraction; this seems quite plausible.

4. Conclusion

The experimental data show that the nature of the substructural changes accompanying high temperature creep of mono- and polycrystalline nickel is determined by the magnitude of the effective stresses. A threshold stress p applies to each testing temperature such that at $p < p_0$ creep occurs mainly by the Nabarro-Herring diffusion mechanism, and at $p > p_0$ by the movement and climb of dislocations. The temperature dependence of p_0 is, to a first approximation, determined by the temperature dependence of the shear modulus.

At $p < p_0$ creep is either accompanied by no structural and substructural changes (in the case of samples which have been thoroughly annealed) or causes enlargement of the blocks and a decrease in the dislocation density. At $p > p_0$ the blocks are crushed and the dislocation density increased.

Regardless of the applied stress, high temperature creep is accompanied by the development of porosity, the appearance of which is clearly observed at the steady-state crepe stage. The mechanism for pore generation under conditions of purely diffusion-creep ($p < p_0$) and dislocation-creep is apparently different. Pore development occurs by a diffusion mechanism.

References

1. B. YA. PINES, *Uspekhi fizicheskikh nauk* **76** (3) (1962) 519 (*Soviet Physics Uspekhi* **5** (2) (1962) 251.
2. F. GAROFALO, "Fundamentals of Creep and Creep-Rupture in Metals", New York: MacMillan, 1965.
3. F. R. N. NABARRO, Report of Conference on Strength of Solids (University of Bristol), July 1947, page 75 (pub. 1948).
4. C. HERRING, *J. Appl. Phys.* **21** (1950) 437.
5. H. UDIN, A. J. SHALER, and J. WULF, *J. Metals* **2** (1949) 186.

6. B. YA. PINES, E. E. BADIYAN, and V. D. MAL'TSEV, *Zavodskaya Laboratoriya* **34** (12) (1968) 1520. (Industrial Laboratory, **34** (1968) 1833.
7. B. YA. PINES, E. E. BADIYAN, A. F. SIRENKO, and D. D. SOLNYSHKIN, *Kristallografiya* **12** (1967) 423. (*Soviet Phys. Crystallog.* **12** (3) (1967) 365.
8. B. YA. PINES, E. E. BADIYAN, and A. F. SIRENKO, *Fiz. Metall. i Metallov.* **29** (1970) 1235.
9. M. A. KRIVOGLAZ and K. P. RYABOSHAPKA, *ibid* **15** (1963) 465. (*Phys. Metals Metallog.* **15** (1963) 14.
10. M. WILKINS and M. O. BARGOUTH, *Acta Metallurgica* **16** (1968) 465.
11. A. H. COTTRELL, "Dislocation and Plastic Flow in Crystals." Oxford: Clarendon Press, 1953.
12. V. A. PAVLOV, "Fizicheskie osnovy plasticheskoi deformatsii metallov" ("Physical Bases of Plastic Deformation of Metals"), Moscow: Izd. Akad. Nauk SSSR, 1962.
13. D. HULL and D. F. RIMMER, *Phil. Mag.* **4** (1959) 673.
14. J. WEERTMAN, *J. Appl. Phys.* **28** (3) (1957) 362.